

# Instability of Anisotropic Fermi Surfaces in Two Dimensions

J. González <sup>1</sup>, F. Guinea <sup>2</sup> and M. A. H. Vozmediano <sup>3</sup>

<sup>1</sup>*Instituto de Estructura de la Materia. Consejo Superior de Investigaciones Científicas. Serrano 123, 28006 Madrid. Spain.*

<sup>2</sup>*Instituto de Ciencia de Materiales. Consejo Superior de Investigaciones Científicas. Cantoblanco. 28049 Madrid. Spain.*

<sup>3</sup>*Departamento de Matemáticas. Universidad Carlos III. Butarque 15. Leganés. 28913 Madrid. Spain.*

(July 7, 2017)

The effect of strong anisotropy on the Fermi line of a system of correlated electrons is studied in two space dimensions, using renormalization group techniques. Inflection points change the scaling exponents of the couplings, enhancing the instabilities of the system. They increase the critical dimension for non Fermi liquid behavior, from 1 to 3/2. Assuming that, in the absence of nesting, the dominant instability is towards a superconducting ground state, simple rules to discern between d-wave and extended s-wave symmetry of the order parameter are given.

75.10.Jm, 75.10.Lp, 75.30.Ds.

Since the appearance of high- $T_c$  materials the quest for non-Fermi liquid (NFL) behavior in two space dimensions has attracted great interest. The emergence of the quantum field theory approach to the study of electronic systems [1] seems to put severe constraints on the possibility of NFL behavior, at least for continuum models. Following Ref. [1] no NFL behavior is to be expected in  $D=2$  provided that the coupling is weak, the interaction is short-ranged, and the Fermi surface is isotropic. On the other hand, Anderson [2] and coworkers support strongly the opinion that Fermi liquid behavior will not occur in  $D=2$  under quite general assumptions, which make use of analogies to 1D behavior. The basis of Anderson's approach is the discrete 2D lattice. On the other hand, it has been proved that the critical dimension for Luttinger liquid behavior in isotropic systems is  $D = 1$  [3].

This paper addresses the role of anisotropy of the Fermi surface in inducing instabilities of the Fermi liquid fixed point in 2D. The cases of an extreme anisotropy due to either nesting or a Van Hove singularity are known to produce drastic changes in the system [4–9]. We study here the effect that a strong anisotropy of the Fermi line can have in a continuum model in the absence of nesting and away from a Van Hove singularity.

In between the case of a circular Fermi surface and the existence of a Van Hove singularity lies the possibility that the Fermi surface has inflection points which separate portions where the curvature has opposite signs, as shown in Fig. 1. This situation takes place for a finite range of fillings, and requires no precise fine tuning of the number of electrons in the system. In particular, for the  $t - t'$  Hubbard model in a square lattice, inflection points at the Fermi surface are present for fillings below the Van Hove point ( $-8t' + 16t'^3/t^2 < \varepsilon_F < -4t'$ , where  $t < 0, t' > 0$ ).

Scattering processes which involve two opposite inflection points are analogous to the enhanced scattering present in nested Fermi surfaces [1]. It can be shown that nesting, in any dimension, is a marginal perturbation. The correction that nesting induces to the bare interaction (in dimensionless units) is of order  $\Lambda^0 \log \Lambda$ , where  $\Lambda$  is the high-energy cutoff [1]. A Van Hove singularity induces similar effects in 2D [9].

In order to study the effects induced by inflection points at the Fermi surface, we first analyze the electron-hole polarizability (the bubble in Fig. 2(a)) for a wavevector  $\mathbf{Q}$  which connects two such points at opposite ends of the center of the Brillouin Zone (BZ). The imaginary part of the diagram,  $\text{Im}\Pi(\mathbf{Q}, \omega)$ , measures the density of electron-hole pairs with energy  $\omega$ . In the case of perfect nesting, each strip of holes of energy  $\omega/2$  below the Fermi level coincides with a strip of electrons at energy  $\omega/2$  above the Fermi level. Hence,  $\text{Im}\Pi(\mathbf{Q}, \omega) \sim |\omega|^0$ , and the corresponding coupling is marginal. Near an inflection point, the states of equal energy no longer fill a straight strip in momentum space. Using a reference frame such that the x-axis is parallel to the Fermi surface, we can write:

$$\begin{aligned}\varepsilon(\mathbf{q}) &\approx v_F q_y + \alpha q_x^3 + \beta q_x^4 \\ \varepsilon(\mathbf{q} + \mathbf{Q}) &\approx -v_F q_y - \alpha q_x^3 + \beta q_x^4\end{aligned}\tag{1}$$

The number of electron-hole pairs of energy  $\omega$  available are given by the region in momentum space which satisfy:  $\omega - d\omega \leq \varepsilon_e(\mathbf{q}) - \varepsilon_h(\mathbf{q} + \mathbf{Q}) \leq \omega$ .

Setting  $q_y \approx \omega/(2v_F)$ , these restrictions imply that the region available is bounded, in the transverse direction, by  $q_x \propto q_y^{1/4} \propto \omega^{1/4}$  (note that the cubic term does not break the correspondence between the equal energy slices at  $\mathbf{q}$  and  $\mathbf{q} + \mathbf{Q}$ ). This implies that  $\text{Im}\Pi(\mathbf{Q}, \omega) \propto |\omega|^{1/4}$ . The previous argument can easily be extended to an arbitrary number of dimensions. An inflection point is characterized by a dispersion relation which is linear in the direction normal to the Fermi surface, cubic in one of the transverse directions, and quadratic in all the others. In  $D$  dimensions, this leads to:

$$\text{Im}\Pi(\mathbf{Q}, \omega) \propto |\omega|^{\frac{D-2}{2} + \frac{1}{4}} \quad (2)$$

Hence, the critical dimension is  $D_c = 3/2$ . The same argument, when applied to the standard  $2k_F$  scattering which connects two opposite points of an isotropic Fermi surface, gives  $\text{Im}\Pi(2k_F, \omega) \propto |\omega|^{(D-1)/2}$ , and the corresponding critical dimension is  $D_c = 1$ , in agreement with Ref. [3].

The preceding analysis shows that inflection points enhance the instabilities of the model. Among the possible broken symmetry ground states, we will assume that superconductivity prevails. The model has no tendency towards ferromagnetism, as the density of states needs not be specially large. A spin density wave, or a charge density wave, of momentum  $\mathbf{Q}$  is possible. The associated gap, however, will only span a small fraction of the Fermi surface, centered around the inflection points. Moreover, only two of the eight possible points of a square lattice will take part in the symmetry breaking. As it is shown below, the system is unstable against anisotropic superconductivity. This instability opens a gap over large regions of the Fermi surface (except at the inflection points). Thus, this instability is a more robust alternative than a spin or a charge density wave.

The possible processes which renormalize the particle-particle scattering are shown in Fig. 2. In a 3D isotropic system with repulsive interactions, they lead to the Kohn-Luttinger instability [10], which gives rise to superconductivity at high angular momenta. Note that this instability is absent in 2D isotropic systems [11]. For short-range interactions, the first and second diagrams in Fig. 2 cancel. This fact implies that pairing, if present, cannot arise from the propagator of a quasiparticle, in a similar fashion to phonon mediated pairing. In that case, superconductivity can be expressed in terms of a diagram like the first one in Fig. 2. If the electrons to be paired and the electrons which give rise to the quasiparticle are the same, diagrams like the first one in Fig. 2 are cancelled, to all orders, by diagrams like the following one in the same figure.

In general, we need to consider the scattering of a pair of electrons of momenta  $\mathbf{k}, -\mathbf{k}$  into  $\mathbf{p}, -\mathbf{p}$ . We label these processes by the angle  $\phi$  between  $\mathbf{k}$  and the x-axis, and  $\mathbf{p}$  and the x-axis,  $\phi'$ . In the following, we will label each point at the Fermi surface by the angular variable,  $\phi$ . The value of the corresponding diagram in Fig. 2(c) is denoted  $\Pi(\phi, \phi')$ .

We first analyze contributions of the type  $\Pi(\phi, \phi)$ . We assume a local electron-electron interaction,  $U$ . Then, using Eq. (1) we have

$$\Pi(\phi, \phi) = -i \frac{U^2}{(2\pi)^3} \int d\omega \int d^2q e^{-\varepsilon(\mathbf{q})/\Lambda} e^{-\varepsilon(\mathbf{q} + \mathbf{Q} + \delta\mathbf{Q})/\Lambda} G(\omega, \mathbf{q}) G(\omega, \mathbf{q} + \mathbf{Q} + \delta\mathbf{Q}) \quad (3)$$

where  $\mathbf{Q} + \delta\mathbf{Q}$  is the vector which connects the point at the Fermi surface with momentum  $\mathbf{k}$  with that at  $-\mathbf{k}$ . The parameter  $\Lambda$  is a smooth cutoff in energies which is used to implement the renormalization group (RG) scheme.

Using the new variables:  $\varepsilon = \varepsilon(\mathbf{q} - \delta\mathbf{Q}/2)$  and  $\bar{\varepsilon} = \varepsilon(\mathbf{q} + \mathbf{Q} + \delta\mathbf{Q}/2)$ , the real part of  $\Pi(\phi, \phi)$  becomes, for the convex part of the Fermi line,

$$\begin{aligned} \text{Re}\Pi(\phi, \phi) &= -\frac{U^2}{(2\pi^2)} \int_0^\infty d\varepsilon \int_0^\infty d\bar{\varepsilon} \left| \frac{\partial(q_x, q_y)}{\partial(\varepsilon, \bar{\varepsilon})} \right| \frac{e^{-\varepsilon/\Lambda} e^{-\bar{\varepsilon}/\Lambda}}{\varepsilon + \bar{\varepsilon}} \\ &= -\frac{U^2}{(2\pi^2)} \frac{1}{v_F \beta^{1/4}} \int_0^\infty dy \sqrt{\frac{f^2}{8\beta} + y} - \frac{f}{\sqrt{8\beta}} \frac{e^{-y/\Lambda}}{y} \end{aligned} \quad (4)$$

where the only dependence on  $\delta\mathbf{Q}$  comes through the curvature:  $f \equiv 12\beta \delta Q_x^2 - 6\alpha \delta Q_x$ . A similar expression holds for the concave part of the Fermi surface, with the same respective limit behaviors at large and small values of the cutoff  $\Lambda$ .

The result (4) can be rescaled as a function of the dimensionless parameter  $\frac{f^2/8\beta}{\Lambda}$ , what allows us to study the relative intensity of the corrections in different zones of the Fermi line. We see that, close to the inflection points ( $f \ll \Lambda$ ), the vertex function reaches maximum values

$$\text{Re}\Pi(\phi, \phi) \sim \frac{\Lambda^{1/4}}{\beta^{1/4}} \quad (5)$$

while for points with  $f \gg \Lambda$

$$\text{Re}\Pi(\phi, \phi) \sim \frac{\Lambda^{1/2}}{|f|^{1/2}} \quad (6)$$

Equation (6) reproduces the  $2k_F$  behavior of the response function of an isotropic Fermi liquid. We observe that the function  $\Pi(\phi, \phi)$  has minima at points where the value of the curvature is a maximum. Its natural period is determined by the symmetry of the Fermi line, which in a square lattice is in general  $\pi/2$ .

By adding  $\Pi(\phi, \phi')$  to the bare particle-particle scattering,  $U$ , we obtain the full irreducible vertex in the Cooper channel. This vertex, when inserted into ladder diagrams like the ones depicted in Fig. 3, gives the possible superconducting instabilities. The ladder summation implicit in Fig. 3 respects the lattice symmetries. We write the irreducible vertex as:

$$\begin{aligned} U + \Pi(\phi_1, \phi_2) = & c_0 + c_1(\cos \phi_1 \cos \phi_2 + \sin \phi_1 \sin \phi_2) \\ & + c_2 \cos 2\phi_1 \cos 2\phi_2 + c_3 \sin 2\phi_1 \sin 2\phi_2 \\ & + c_4 \cos 4\phi_1 \cos 4\phi_2 + c_5 \sin 4\phi_1 \sin 4\phi_2 + \dots \end{aligned} \quad (7)$$

The effective interaction in the Cooper channel  $\Gamma(\phi_1, \phi_2)$  has a similar expansion, with coefficients  $\Gamma_n$  whose cutoff dependence is given by:  $\Gamma_n = c_n/(1 - c_n/(4\pi) \log(\Lambda/\Lambda_0))$ . Pairing instabilities are associated to negative values of the  $c_n$ 's in Eq. (7).

Let us now assume that the expansion of  $\Pi(\phi, \phi')$  in angular harmonics can be truncated at fourth order, as shown in Eq. (7). Then, from Eqs. (5) and (6), we can write:  $\Pi(\phi, \phi) \approx a + b \sin^2 4\phi$ , where:  $a \sim O(\Lambda^{1/2}/f^{1/2})$  and  $b \sim O(\Lambda^{1/4}/\beta^{1/4})$ , so that:

$$\begin{aligned} c_0 + c_1 + c_2 + c_4 - U & \sim O(\Lambda^{1/2}/f^{1/2}) \\ c_3 - c_2 & \sim 0 \\ c_5 - c_4 & \sim O(\Lambda^{1/4}/\beta^{1/4}) \end{aligned} \quad (8)$$

In order to close this system of equations, we compute  $\Pi(-\phi, \phi)$ . This function is  $\sim O(\Lambda^{1/2}/f^{1/2})$  if  $\phi = \pi n$  and shows a crossover to a behavior  $\sim O(\Lambda)$  for other values of  $\phi$ . Hence,  $\Pi(\phi, -\phi) \approx c + d \cos^2 \phi$ , where:  $c \sim O(\Lambda)$  and  $d \sim O(\Lambda^{1/2}/f^{1/2})$ . It implies that:

$$\begin{aligned} c_0 - c_1 - c_3 - c_5 - U & \sim O(\Lambda) \\ 2c_1 & \sim O(\Lambda^{1/2}/f^{1/2}) \\ c_2 + c_3 & \sim 0 \\ c_4 + c_5 & \sim 0 \end{aligned} \quad (9)$$

From (8) and (9) we obtain that the dominant modes in the limit  $\Lambda \rightarrow 0$  are  $c_0 - U \sim -c_4 \sim c_5 \sim O(\Lambda^{1/4}/\beta^{1/4})$ . Hence,  $c_4$  is the only negative coefficient to that leading order and the system has an instability towards extended s-wave pairing, with a gap which has two nodes in each quadrant of the BZ. We stress that this argument follows the standard BCS procedure, reformulated in RG language. The only approximation involved is the truncation of the expansion (7) to fourth order.

We can extend the previous analysis to anisotropic Fermi surfaces without inflection points, like the round shaped one shown in Fig. 1, at the other side of the Van Hove filling. Then, the vertex  $\Pi(\phi, \phi)$  is always  $\sim O(\Lambda^{1/2}/f^{1/2})$  but it is modulated by the local curvature of the Fermi surface. Hence,  $\Pi(\phi, \phi)$  has maxima for  $\phi = \pi/4$  and equivalent points, where the curvature reaches its minimum value. The same argument gives that the minima of  $\Pi(\phi, \phi)$  lie at  $\phi = 0$  and equivalent points. The vertex is modulated by  $\Pi(\phi, \phi) \approx a + b \sin^2 2\phi$ , where:  $a \sim b \sim O(\Lambda^{1/2}/f^{1/2})$ . A similar analysis to that applied above leads to the conclusion that  $c_2$  is now the dominant coefficient that becomes negative, implying a superconducting instability with  $d_{x^2-y^2}$  symmetry, in agreement with previous calculations for Fermi surfaces of similar shapes [12].

We have assumed that the shape of the Fermi surface does not change much upon lowering the cutoff,  $\Lambda$ . This is the case if only the electrons near the Fermi surface are affected by the interaction, that is,  $\Lambda \sim U \ll E_F$ , where  $E_F$  is the Fermi energy. Different superconducting instabilities may arise in dilute systems where this approximation is not valid [11].

In conclusion, we have extended the standard renormalization group treatment of interacting electrons to systems with strongly anisotropic Fermi surfaces. We have shown that the existence of inflection points change the scaling properties of the interactions. The critical dimension which signals non-Fermi liquid behavior is  $3/2$ . The superconducting vertex, near the inflection points, also changes its scaling properties. This feature allows us to propose a simple scheme to analyze the possible superconducting instabilities of the system (the Kohn-Luttinger mechanism). We have extended the analysis to other anisotropic Fermi surfaces in the square lattice. The superconducting order

parameter is determined by the modulation of the curvature around the Fermi surface. When the curvature has two zeros in each quadrant of the BZ, we find extended s-wave pairing. The gap has two nodes in each quadrant of the BZ. If the curvature shows only one minimum, we obtain d-wave pairing, which can be  $x^2 - y^2$ , if the region of minimum curvature is along the diagonal of the BZ, or of the  $xy$  type, if the minimum of curvature is along the axes. In all cases, the gap has a maximum in the region of maximum curvature of the Fermi surface. This region has the lowest density of states. It is interesting to note that a *screening* diagram, like the first one in Fig. 2, favors a gap which spans regions of high density of states. An unusual feature of the Kohn-Luttinger instability is that it is induced by an *antiscreening* diagram, the third in Fig. 2.

For the particular case of the  $t - t'$  Hubbard model, we propose a phase diagram with extended s pairing for fillings below the Van Hove singularity, and  $d_{x^2-y^2}$  for fillings above it. At the Van Hove filling the system shows magnetic instabilities. Different approximations indicate that the ferromagnetic instability is dominant for a finite range of parameters [13]. For values of  $t'$  below the ferromagnetic regime, though, a finite window for superconductivity with  $d_{x^2-y^2}$  order parameter develops, as confirmed by a numerical diagonalization approach [14].

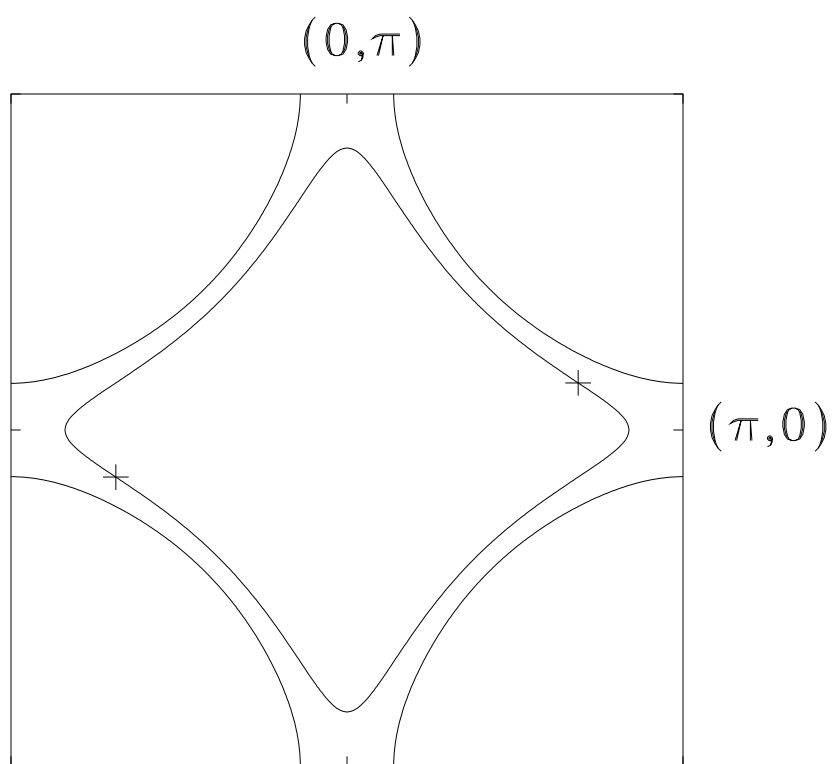
The closeness of a transition towards a d-wave and an extended s-wave superconductor found here implies that, in the absence of perfect tetragonal symmetry, a mixture of the two is likely [15]. Such a possibility is consistent with recent photoemission experiments in the overdoped regime of BiSCCO [16]. Alternative scenarios for the interplay between the d-wave and extended s-wave symmetry of the order parameter have been proposed invoking different effective interactions [17–19]. The framework presented in this Letter, on the other hand, links in a natural fashion the symmetry of the order parameter to the shape of the Fermi surface. Finally, our study can be relevant for the 2D anisotropic superconductor  $\text{Sr}_2\text{RuO}_4$  [20], which is well into the weak coupling regime and has a superconducting state that influences a narrow energy range near the Fermi level (see, however, Ref. [21]).

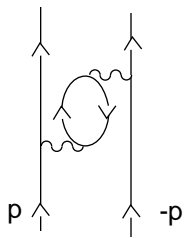
- 
- [1] R. Shankar, Rev. Mod. Phys. **66**, 129 (1994). J. Polchinski in *Proceedings of the 1992 TASI in Elementary Particle Physics*, J. Harvey and J. Polchinski eds., World Scientific (Singapore) 1992. A. C. Hewson, Adv. Phys. **43**, 143 (1994).
  - [2] P. W. Anderson, Phys. Rev. Lett. **64**, 1839 (1990); *ibid* **65**, 2306 (1990).
  - [3] K. Ueda and T. M. Rice, Phys. Rev. B **29**, 1514 (1984). C. Castellani, C. Di Castro and W. Metzner, Phys. Rev. Lett. **72**, 316 (1994). W. Metzner, C. Castellani and C. di Castro, preprint (cond-mat/9702012).
  - [4] H. J. Schulz, Europhys. Lett. **4**, 51 (1987).
  - [5] J. E. Dzyaloshinskii, Pis'ma Zh. Eksp. Teor. Fiz. **46**, 97 (1987) [JETP Lett. **46**, 118 (1987)].
  - [6] P. A. Lee and N. Read, Phys. Rev. Lett. **58**, 2691 (1988).
  - [7] R. S. Markiewicz, J. Phys. Condens. Matter **2**, 665 (1990). R. S. Markiewicz and B. G. Giessen, Physica (Amsterdam) **160C**, 497 (1989).
  - [8] C. C. Tsuei *et al.*, Phys. Rev. Lett. **65**, 2724 (1990). P. C. Pattnaik *et al.*, Phys. Rev. B **45**, 5714 (1992).
  - [9] J. González, F. Guinea and M. A. H. Vozmediano, Europhys. Lett. **34**, 711 (1996); Nucl. Phys. B **485**, 694 (1997).
  - [10] W. Kohn and J. M. Luttinger, Phys. Rev. Lett. **15**, 524 (1965).
  - [11] M. A. Baranov, A. V. Chubukov and M. Yu. Kagan, Int. J. Mod. Phys. **B6**, 2471 (1992).
  - [12] D. Zanchi and H. J. Schulz, Phys. Rev. B **54**, 9509 (1996).
  - [13] S. Sorella, R. Hlubina and F. Guinea, Phys. Rev. Lett. **78**, 1343 (1997).
  - [14] J. González and J. V. Alvarez, preprint (cond-mat/9609162), to be published in Phys. Rev. B.
  - [15] J. Betouras and R. Joynt, Europhys. Lett. **31**, 119 (1995). Q. P. Li, B. E. C. Koltenbah and R. Joynt, Phys. Rev. B **48**, 437 (1993). G. Kotliar, Phys. Rev. B **37**, 3664 (1988). A. E. Ruckenstein, P. J. Hirschfeld and J. Apel, Phys. Rev. B **36**, 857 (1987).
  - [16] J. Ma *et al.*, Science **267**, 862 (1995). R. J. Kelley *et al.*, Science **271**, 1255 (1996).
  - [17] D. Duffy *et al.*, preprint (cond-mat/9701083).
  - [18] A. Perali *et al.*, Phys. Rev. B **54**, 16216 (1996).
  - [19] A. A. Abrikosov, Phys. Rev. B **52**, 15738 (1995).
  - [20] Y. Maeno *et al.*, Nature **372**, 532 (1994). T. Yoyoka *et al.*, Phys. Rev. Lett. **75**, 3009 (1996).
  - [21] D. F. Agterberg, T. M. Rice and M. Sigrist, preprint (cond-mat/9702148). I. I. Mazin and D. Singh, preprint (cond-mat/9703068).

FIG. 1. Different shapes of the Fermi line for the  $t - t'$  Hubbard model about the Van Hove filling. Two opposite inflection points are marked on the figure.

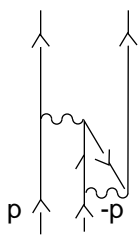
FIG. 2. Total interaction vertex in the BCS channel.

FIG. 3. Ladder summation in the BCS channel used to describe the possible superconducting instabilities of the system.

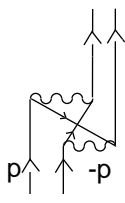




(a)



(b)



(c)

A diagrammatic equation. On the left is a shaded gray oval with two black dots (vertices) on its horizontal boundary. The top arc has an arrow pointing right, and the bottom arc has an arrow pointing left. This is followed by an equals sign. To the right of the equals sign is a white oval with two black dots on its horizontal boundary. The top arc has an arrow pointing right, and the bottom arc has an arrow pointing left. This is followed by a plus sign. To the right of the plus sign is a diagram consisting of a white oval with two black dots on its horizontal boundary (top arrow right, bottom arrow left) immediately followed by a shaded gray oval with two black dots on its horizontal boundary (top arrow right, bottom arrow left).